SHAKING TABLE MODEL TESTS ON REINFORCED SOIL RETAINING WALLS BY USING NEWLY-DEVELOPED GEOCELL REINFORCEMENTS AND GEOGRID REINFORCEMENTS

Xinye HAN[1], Tomoharu MERA[2], Takashi KIYOTA[3] and Toshihiko KATAGIRI[4]

ABSTRACT: In order to improve the seismic performance of GRS RWs, a new type of geocell, called square-shaped geocell having straight longitudinal members with transversal walls at separated locations was developed. The results of previous pullout tests have clearly shown the effectiveness of newly-developed geocell (square-shaped geocell) to achieve a higher pullout resistance than both conventional-type geocell (diamond-shaped geocell) and ordinary geogrid. In this paper, to check whether square-shaped geocell reinforced soil retaining wall has a substantially high seismic stability against a large seismic load, two shaking table model tests on reinforced soil retaining walls by using square-shaped geocell models and geogrid models backfilled in sandy soil were carried out. And a gravity-type retaining wall model was also tested for comparison. It is found that square-shaped geocell reinforced soil retaining wall model exhibited higher seismic performance than geogrid reinforced soil retaining wall model and gravity-type retaining wall model from the evaluation of residual sliding displacement of the wall facing, residual overturning angle of the wall facing, settlements of the backfill and response acceleration of the wall facing. In addition, the determination of critical acceleration was also discussed.

Key Words: Shaking table model tests, geocell, geogrid, residual displacement, critical acceleration

INTRODUCTION

For the last two decades, geosynthetic-reinforced soil retaining walls (GRS RWs) with a stage-constructed full-height rigid (FHR) facing have been constructed for railways, highways and other facilities and have shown greater seismic resistance than conventional retaining wall structures (Tatsuoka et al., 2009). Geogrids are commonly used as planar reinforcements to tensile-reinforce the backfill of RWs, embankments and other soil structures.

However, GRS RWs with geogrids may encounter the following potential problems: 1) for ordinary structures, the local soil materials which may be poorly graded or include larger particles would be inevitably used as backfill. This would result in a decrease in its deformability. On the other hand, to obtain a high friction resistance with geogrids, the backfill soil is restricted to sandy soil and heavy

[1] Graduate student, Institute of Industrial Science, University of Tokyo
[2] Graduate student, Institute of Industrial Science, University of Tokyo
[3] Associate professor, Institute of Industrial Science, University of Tokyo
[4] Technical director, Institute of Industrial Science, University of Tokyo

compaction work should be conducted which lead to an increase in construction cost; 2) for some important structures such as high-speed railways, the requirement of seismic stability and allowable deformation of GRS RWs are higher than ordinary structures, which requires the reinforcement to have a higher resistance. In order to alleviate these problems and improve the seismic performance of GRS RWs, a new type of geocell (Fig. 1a) was developed by Han et al. (2013), which has a different cell shape compared with traditional type geocell (diamond-shaped geocell, Fig. 1b), called square-shaped geocell having straight longitudinal members with transversal walls at separated locations. The pullout test results indicated that square-shaped geocell showed only slightly progressive deformation and therefore showing higher pullout resistance and initial stiffness than diamond-shaped geocell. What's more, Han et al. (2013) conducted a series of pullout tests using square-shaped geocell models and a prototype geogrid (Tensar SS-35) embedded in gravelly soils having different particle sizes indicating the important benefit of square-shaped geocell which can confine large soil particles in their three dimensional cells and respective cells provide large anchorage capacity when pull laterally compared with geogrids. In this paper, the seismic performance of GRS RWs reinforced by square-shaped geocell models and geogrid models was evaluated by two shaking table model tests. In addition, a gravity-type retaining wall model was also tested for comparison.

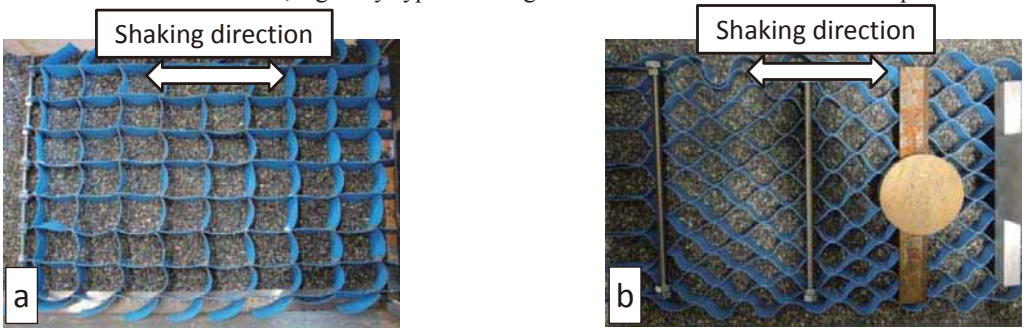

Figure 1. a) Square-shaped geocell model; b) Diamond-shaped geocell model

SHAKING TABLE TEST

Model configurations and testing materials

General

The model tests were carried out by using a shaking table at IIS, the University of Tokyo. In total three types of small-scaled retaining wall models were constructed in a 40cm-wide by 180cm-long and 87.5cm-high rigid soil container fixed to the shaking table. Both front and back side of this container comprised transparent-tempered glass windows to make the deformation behavior of model visible. Figs. 2, 3 and 4 show the cross-sections of three different retaining wall models which are 39.5cm in width. They consisted of one gravity-type RW and two types of reinforced-soil RWs with a FHR facing having two different types of reinforcements (geocell model reinforcements and geogrid model reinforcements). The total height of retaining wall models was 50 cm assuming a scale down factor of 1/10. The gravity-type RW was constructed by a FHR facing (39.5 cm-wide× 45 cm-high× 4.5 cm-thick) connected with a spread-footing foundation (39.5 cm-wide× 5 cm-high× 20 cm-thick). A FHR facing for reinforced-soil RWs was prepared having a size of 39.5 cm in width, 50 cm in height and 3 cm in thickness. All of these walls were made of duralumin. The back faces of gravity-type RW, and the bottom surfaces of the foundation directly contact with the subsoil, and the back faces of FHR facings for geogrid-reinforced RW and geocell-reinforced RW were made rough by being covered with a sheet of sand paper (No. 150). In order to minimize the friction between the edge of RW models and the side wall of the soil box, a sponge tape and grease were used, and the leakage of sand from the gap between RW models and the soil container could completely be prevented.

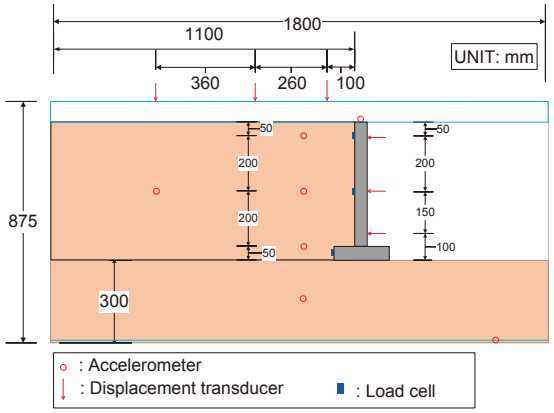

Figure 2. Schematic diagram of gravity-type RW model

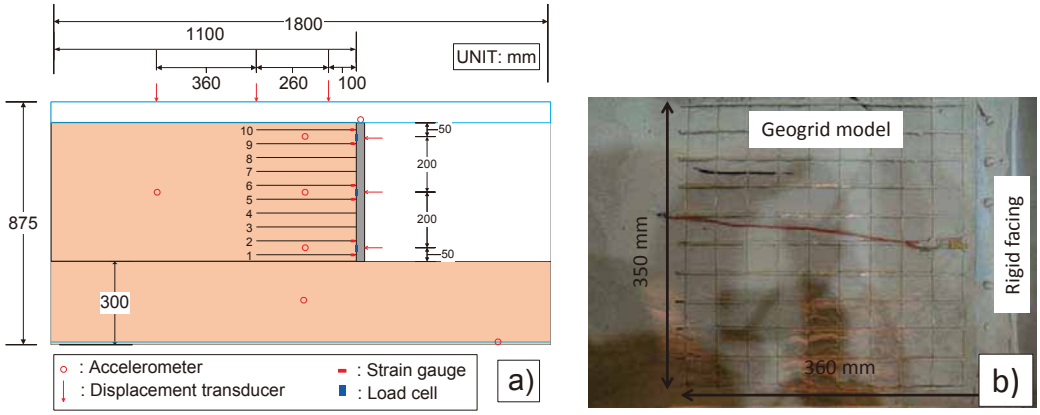

Figure 3. a) Schematic diagram of geogrid-RS RW model; b) geogrid model connected to facing

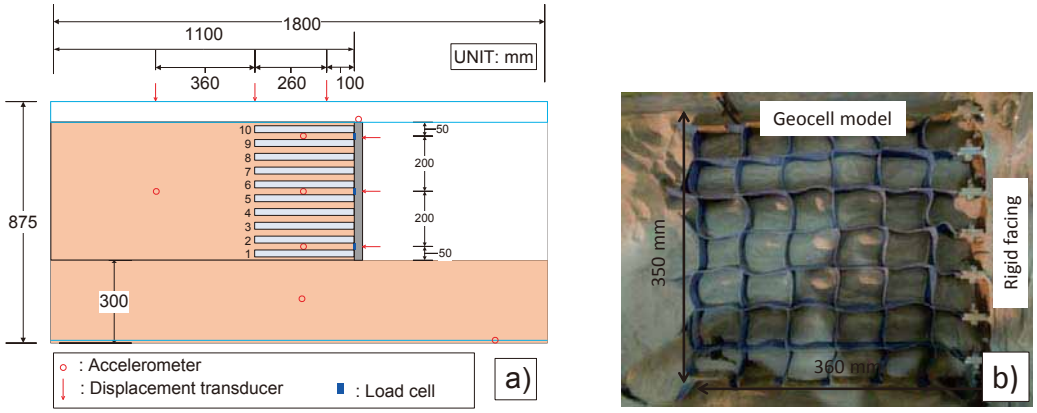

Figure 4. a) Schematic diagram of geocell-RS RW model; b) geocell model connected to facing

Backfill soil and subsoil

As shown in Figs. 2, 3a and 4a, the thickness of subsoil was 30 cm. The subsoil and backfill soil were produced by pluviating air-dried Silica No.7 sand (D_{50}=0.25 mm; U_c=2.2) to obtain a relative density about 90%. To capture the deformation of the backfill throughout the shaking tests, thin horizontal layers with a width of about 0.5 cm of black-dyed Silica sand were placed at a vertical spacing of 10 cm immediately behind the front transparent glass window of sand box. In addition, a number of rivets made of aluminum with a black circular flat edge were used as targets set in the backfill soil adjacent to the transparent glass window at a horizontal spacing of 5 cm and a vertical spacing of 5 cm for the purpose of measuring deformation of the backfill on plane strain condition. In order to ensure permanent contact between the glass and the targets, thereby following the surrounding sand movement, silicon grease was smeared between the targets and the glass.

After filling the sand, a surcharge of 1 kPa was applied by placing lead shots on the surface of the backfill to simulate the weight of the road base for structures or traffic.

Reinforcements

For geogrid-RS RW model (Fig. 3), geogrid reinforcements used in actual field cases were simulated by a set of regular grids comprising longitudinal members (made of thin and narrow phosphor-bronze strips, 0.2mm-thick and 3mm-wide) welded at nodes to transversal members (made of mild steel bar, 0.5mm in diameter) at intervals of 35 mm. To effectively mobilize friction between the reinforcement and the backfill, sand particles were glued on the surface of the strips. Strain gauges were attached to the reinforcements to measure the tensile force. The geogrid model reinforcement was 360 mm (length) × 350 mm (width).

For geocell-RS RW model (Fig. 4), the square-shaped geocell model reinforcement was also set to 360 mm (length) × 350 mm (width), having six square cells in the longitudinal direction and seven square cells in the transverse direction. The height of transverse member is 25mm and the size of each cell is 60mm×50mm. It is made from polyester (PET) covered with PVC for protection which is a relative weak material can be used in scaled-down model test (Kongkitkul et al., 2007). Ten layers of reinforcements were horizontally placed at a vertical spacing of 5 cm in the backfill which was set by reducing them to a scale of one-tenth that of actual reinforced soil retaining walls with a full-height rigid facing constructed in Japan (R.T.R.I., 2000). Note that the geometric shape and arrangement of reinforcements were determined by referring to those actual one, while the similitude on the properties of geogrid materials was not considered for the purpose of measuring tensile force. The reinforcement connections with the facing panel were designed to be perfectly rigid to prevent slippage of the reinforcement layers at the facing (Figs. 3b and 4b).

Instrumentation and base excitation

The accelerations and deformations were measured using accelerometers and displacement transduces such as laser sensors and LVDT sensors, respectively. From Figs. 2a, 3a and 4a, the acceleration sensors were positioned at predefined locations during layer by layer construction of the reinforcements. One accelerometer was attached to the container base to measure base acceleration, and another accelerometer was attached to the top of the wall to measure response acceleration. The response accelerations of reinforced backfill zone were measured by three accelerometers from top to bottom, and the last accelerometer was positioned at the unreinforced backfill zone. Facing deformation was measured using laser sensors attached to rigid bars which were fastened to the soil container. Deformation of the facing was measured at three points from top to bottom as shown in Figs. 2a, 3a and 4a. The settlements of the backfill behind the wall were also measured using three vertical LVDT sensors connected to the soil container frame with stiff beams. To isolate the friction effect of side wall, all parameters were measured at the middle of the physical model on a line parallel to the side wall. The data from all instrumentation were collected at a high sampling rate (100 Hz) to avoid aliasing errors and to capture the peak values of dynamic wall response during base excitation.

Each retaining wall models was subjected to harmonic sinusoidal base acceleration motion at predominant frequency of 5 Hz having twenty cycles per stage. The acceleration amplitude was increased stage by stage with a target increment of 100 gal from 100 gal to until the failure or collapse

occurs (Fig. 5).

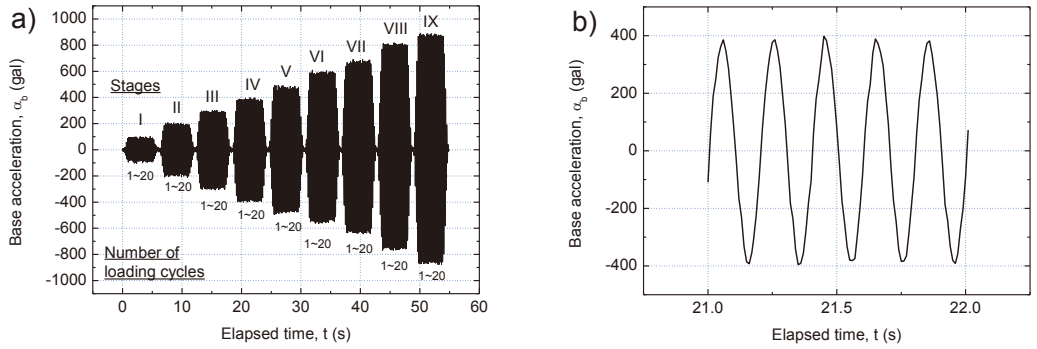

Figure 5. Input base acceleration characteristics: a) base input acceleration; b) one-second window

RESULTS AND DISCUSSIONS

Failure pattern of models

Figure 6 shows the residual displacement of the wall and the residual deformation of the backfill, which were observed at the end of the final shaking step. It can be seen that the predominant failure type for all three cases was overturning, associated with some small component of sliding failure. For the gravity-type RW, brittle failure occurred during the base acceleration of 488 gal and a single failure plane was formed starting from the heel of the wall. For the geogrid-RS RW and geocell-RS RW, similar ductile failure patterns were observed during the base acceleration of 790 gal and 877 gal, respectively, which indicated that geocell-RS RW has a higher seismic performance than geogrid-RS RW as well as gravity-type RW. In addition, the reinforced backfill suffered simple shear deformation along horizontal planes (Watanabe et al., 2003; Nakajima et al., 2010), and two differently inclined failure planes developed simultaneously in the unreinforced backfill zone while the development of the failure planes may originated from the position between Layer 1 and Layer 2 (shown in Figs. 3a, 4a and 6) not the bottom of the reinforced wedge, indicating that the bottom layer of reinforcements may restricted the sliding of the wall, which will be discussed hereafter.

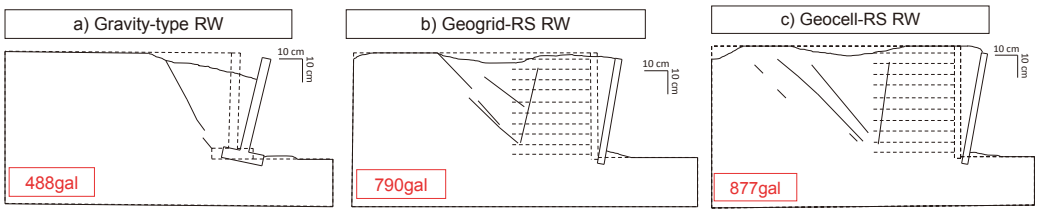

Figure 6. Residual deformation of wall at failure state: a) gravity-type RW; b) geogrid-RS RW; c) geocell-RS RW

Residual displacements of wall and settlements of backfill

Representative residual displacements of walls in terms of base sliding, d_s, overturning angle, θ, and settlements at the crest of backfill, S_{10} and S_{36}, after each shaking step were plotted in Fig. 7 versus the base acceleration. As shown in Figs. 2, 3a and 4a, the base sliding was measured at the height of 5 cm from the bottom of the facing. The overturning angle was measured and calculated from the lateral displacements at the top and bottom of the facing. The settlements, S_{10} and S_{36}, were measured at the crest of backfill at 10 cm and 36 cm from the back of facing, respectively.

As can be seen in Figs. 7 and 8, up to a base acceleration value of around 350 gal no significant difference could be observed. However, under higher base accelerations, the residual wall displacements accumulated rapidly with gravity-type RW. In contrast, the geogrid-RS RW and geocell-RS RW exhibited more ductile behavior, particularly geocell-RS RW showed smaller residual overturning angle and settlements for increasing base acceleration indicating a higher resistance against seismic loading. For example, during a base acceleration value of about 500 gal, the geogrid-RS RW had a overturning angle around 1.3 degrees, while the geocell-RS RW had only a overturning angle around 0.4 degrees.

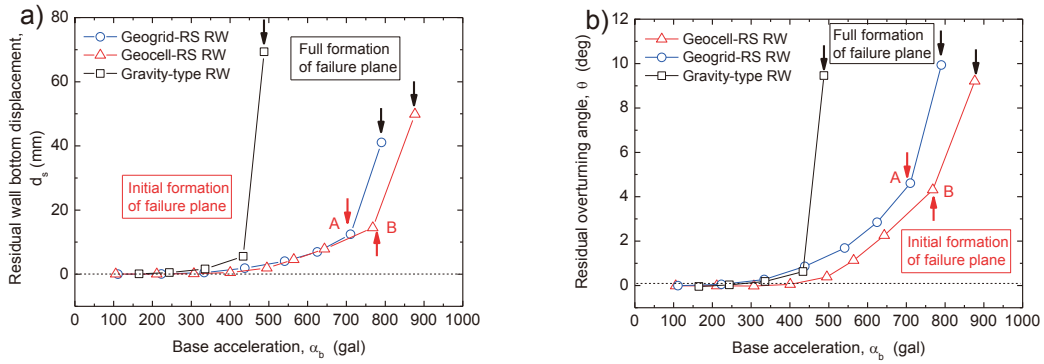

Figure 7. Comparisons of residual displacements of wall: a) residual sliding displacement; b) residual overturning angle, against base acceleration

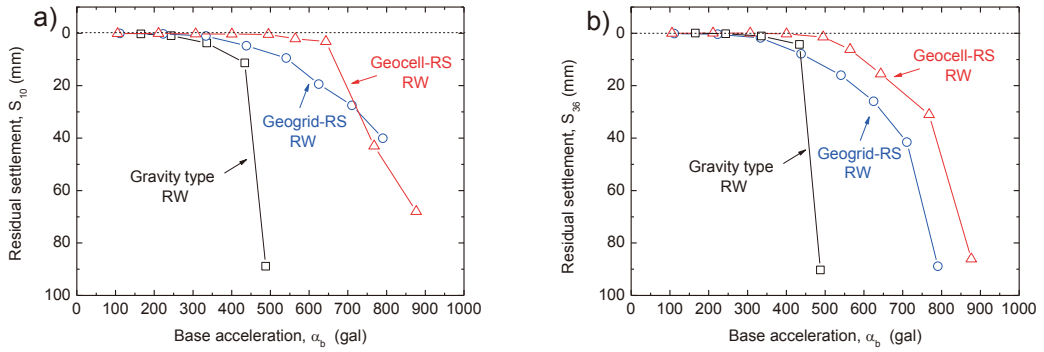

Figure 8. Residual settlements of backfill at: a) 10 cm and b) 36 cm from back of the facing, against base acceleration

It is interesting to note that, the sliding displacement of geogrid-RS RW and geocell-RS RW were the same each other until a base acceleration value of around 700 gal, after which a larger sliding displacement of geogrid-RS RW occurred (Fig. 7a). While the overturning angle of geocell-RS RW was always smaller than that of geogrid-RS RW from a base acceleration value of around 200 gal (Fig. 7b). This is due to the fact that the sliding displacement of wall was mainly induced by the shear deformation of the subsoil beneath the reinforced backfill, and overturning of the wall was mainly induced by the shear deformation of the reinforced backfill (Nakajima et al., 2010). In this study, the subsoil conditions were the same for the two model tests resulting in the same sliding displacement before initial failure plane were formed (points at A and B shown in Fig. 7a), after which the bottom layer of reinforcement may restrict the sliding of the wall, which induced different sliding displacements. On the other hand, the geocell reinforcements may provide larger mobilized resistances in the reinforced backfill zone, which increased the stability of reinforced backfill, thereby a smaller

overturning of the geocell-RS RW occurring compared with geogrid-RS RW.

Critical acceleration

Critical acceleration is important as a measure of stability after which the dynamic factor of safety will be less than one, and permanent displacement will be induced. As shown in Fig. 7, for gravity-type RW, the displacement-acceleration curves were bi-linear clearly. That is, deformation was small until 434 gal, after which deformation was suddenly increased. Thus the value of 434 gal could be considered the model specific critical acceleration value.

However, the determination of critical accelerations for geogrid-RS RW and geocell-RS RW is not so clear, since they showed a gradual increase in the displacements as the increase of base acceleration. In this study, the critical accelerations of geogrid-RS RW and geocell-RS RW were determined at the time when the initial failure plane was observed in the backfill, which were indicated as the red vertical arrows in Fig. 7. Thus, for geogrid-RS RW and geocell-RS RW, the critical accelerations were 711 gal and 768 gal, respectively, after which the displacement increased sharply associated with progressive failure until the full formation of the failure planes at 790 gal and 876 gal (black vertical arrows shown in Fig. 7), respectively. Note also that the determined critical accelerations generated a cumulative displacement of 8.18% of the wall height for geogrid-RS RW and 7.53% for geocell-RS RW which were calculated at the top of model walls. Table 1 summarized both the timings of initial and full formation of failure planes based on observation, showing that geocell-RS RW has a higher seismic performance than geogrid-RS RW and gravity-type RW in terms of strength (i.e. base acceleration at the time of formation of failure) and corresponding deformation characteristics (top wall displacement).

Table 1. Dynamic characteristics of retaining wall at the time of formation of failure plane

		Gravity-type RW	Geogrid-RS RW	Geocell-RS RW
Initial formation of failure plane	Base acceleration (B)	434gal (A)	711gal	768gal
	Residual displacement at top of wall	1.1% × H (A)	8.18% × H	7.53% × H
Full formation of failure planes	Base acceleration	488gal	790gal	877gal
	Residual displacement at top of wall	16.7%× H	17.5%× H	16.2%× H

A) Obtained based on displacement- base acceleration curve
B) Defined as critical acceleration
H: Height of wall

Model wall acceleration response

Amplification of acceleration is a design concern because it can generate larger accelerations leading to larger destabilizing dynamic earth pressure and wall inertia. The acceleration amplification factors at top of the facing wall and at the depth of 5 cm in the reinforced soil zone (Fig. 2, 3a, and 4a) can be calculated by dividing the outward peak acceleration amplitude by the corresponding base peak acceleration amplitude. The results of these calculations are plotted versus base acceleration amplitude in Fig. 9.

The gravity-type RW exhibited a general trend of increasing amplification with increasing base acceleration, with highest facing wall amplification factor of 1.88 occurring during the final shaking step of 488 gal at failure. However, for geogrid-RS RW and geocell-RS RW, the amplification factors increased with increasing base acceleration until the highest facing wall amplification factors of 2.10 and 2.07 occurring during the shaking steps of 711 gal (point A in Fig. 9a) and 643 gal (point C in Fig. 9a) at which initial failure plane has already formed or just started to form. After this, the amplification factors decreased. In other words, prior to the estimated critical acceleration value (points at A and B in Figs. 9a) in the cases of geogrid-RS RW and geocell-RS RW the amplification factors increased as the base acceleration increased but decreased thereafter. This is likely related to formation of failure

plane in the unreinforced backfill associated with the change of stiffness in the soil, the damping capacity of the soil-wall system, and the fundamental frequency of the soil and soil-wall system, which is not the subject of this paper.

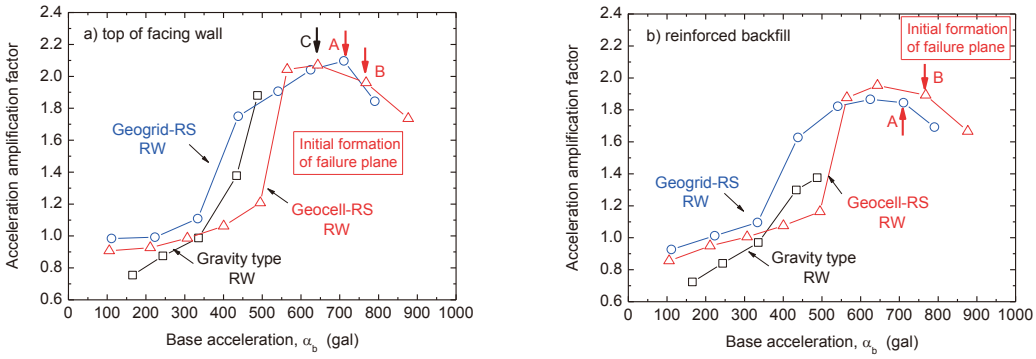

Figure 9. Acceleration amplification factors at: a) top of facing wall and b) at depth of 5 cm in the reinforced backfill zone

Figure 9b also demonstrated that the amplification factor of geocell-RS RW in the reinforced backfill zone was lower than that of geogrid-RS RW before the value of base acceleration around 550 gal indicating a higher shear stiffness of geocell-RS RW due to the larger mobilization of tensile force of geocell reinforcement. Note also that, the amplification factor increased suddenly at the base acceleration of 400gal for geogird-RS RW and 550 gal for geocell-RS RW, respectively, which suggested that the reinforcements at the top (i.e. Layer 10 shown in Figs. 3a and 4a)were pulled out from backfill soil. Finally, by comparison of the amplification factors at the top of wall and at the depth of 5 cm in the reinforced soil zone, it is found that the trends of amplification response were similar but the latter showed a smaller value of amplification factor. This is indicative of a possible phase difference in deformation-time response between the rigid wall facing and the backfill soil.

CONCLUSIONS

A new type of geocell, called square-shaped geocell, was developed to improve the seismic performance of GRS RWs. Three shaking table model tests on gravity-type RW, geogrid-RS RW and geocell-RS RW backfilled in sandy soil were conducted. The main conclusions and future plans from this study are as follows:

1) The geocell-RS RW exhibited higher seismic performance than geogrid-RS RW and gravity-type RW from the evaluation of residual displacements and response acceleration of the wall.
2) For gravity-type RW, the critical acceleration can be determined from the residual displacement-acceleration curves which are bi-linear clearly. For geogrid-RS RW and geocell-RS RW, the critical acceleration was determined based on the formation of initial failure plane. And the value of critical acceleration for geocell-RS RW (768 gal) was larger than that of geogrid-RS RW (711 gal) and gravity-type RW (434 gal).
3) However, the formation of initial failure plane should be evaluated more precisely from the image analysis in the future.
4) To evaluation the dynamic stability of different types of retaining walls, not only should be evaluated the strength of a given retaining wall (i.e. acceleration amplification factor), but also the stiffness and damping capacity should also be checked.

ACKNOWLEDGMENT

The author sincerely appreciates the help of Mr. Michiyuki HARATA in TOKYO PRINTING INK MFG. CO., LTD to provide the geocell models, which can make the experiments proceeding smoothly.

REFERENCES

Han, X., Kiyota, T. and Tatsuoka, F. (2013). "Pullout resistance of geocell placed as reinforcement in gravelly soil backfill." *Proc. of the 10th International Conference on Urban Earthquake Engineering*, Tokyo Institute of Technology, Tokyo, Vol.1, 533-538.

Han, X., Kiyota, T. and Tatsuoka, F. (2014). "Comparison of pullout behaviors between geogrid and a newly-developed geocell." *Proc. of 10th International Conference on Geosynthetics*, Berlin. (Submitted).

Kongkitkul, W., Hirakawa, D. & Tatsuoka, F. 2007. "Viscous behaviour of geogrids; experiment and simulation." *Soils and Foundations*, 47, No. 2, 265-283.

Nakajima, S., Koseki, J., Watanabe, K., Tateyama, M. 2010. "Simplified procedure to evaluate earthquake-induced residual displacement of geosynthetic reinforced soil retaining walls." *Soils and Foundations*, 50, No. 5, 659-678.

Railway Technical Research Institute. 2000. *Railway structure design standard for earth structures (SI unit version)*, Maruzen, 158-159 (in Japanese).

Tatsuoka, F., Koseki, J., and Tateyama, M. (2009). "Seismic behaviour of geosynthetic-reinforced structures: Lessons from recent earthquakes and from recent earthquakes and design approaches." *The 12th Italian Conference on Geosynthetics*, Italy.

Watanabe, K., Munaf, Y., Koseki, J., Tateyama, M. and Kojima, K. 2003. "Behaviors of several types of model retaining walls subjected to irregular excitation. " *Soils and Foundations*, Vol.43, No.5, 13-27.